

ULTRASOUND-BASED NON-INVASIVE INTRACRANIAL PRESSURE

Chiara Robba
January 2018

**University of Genova, PhD Course in Neurosciences Curriculum Neuroscienze Cliniche e
Sperimentali (XXX Ciclo)**



This dissertation is submitted for the degree of Doctor of Philosophy

ACKNOWLEDGMENT

I acknowledge the University of Genoa and the Department of Neuroscience for this great opportunity, in particular Prof. Antonio Uccelli, Abruzzese and Prof. Gianluigi Mancardi.

Every single step of this thesis wouldn't have been possible without the help, support and professionalism of Prof. Marek Czosnyka and the Brain Physics Laboratory, Addenbrooke's Hospital, Cambridge. I remember the daily coffees in Prof. Czosnyka's office talking about research as the most incredible moments of my career; he and his group believed in me when I was just a student and held my hand thorough this long and wonderful journey in Cambridge; they have been a family for me and I own these people everything. In particular many thanks to: Danilo Cardim, Joseph Donnelly, Zofia Czosnyka, Peter Smielwski, Manuel Cabeleira, Mary Xiuyun Liu.

I was lucky enough to have the support of a great team of academic professionals over the last 4 years; Prof. David Menon, Prof. Arun Gupta, Prof. Peter Hutchinson, and the clinical team I have been working with: Dr Andrea Lavinio, Dr Basil Matta, Dr Ari Ercole, Dr Rowan Burnstein, Dr Jonatan Coles, Dr Ronan O'Leary, Dr Derek Duane and all the staff of the Neurocritical Care Unit at Addenbrooke's Hospital, Cambridge.

Thank you to Dr Mypinder Sekhon and Marcel Aries who are and have been an inspiration.

I also have to thank many Italian friends: Susanna Bacigaluppi, Nicola Bragazzi, Dr Frank Rasulo, Dr Rita Bertuetti, Dr Marco Lattuada, Prof. Pelosi, Prof. Citerio, Prof. Bilotta, Prof. Latronico.

Least but not last, thank you very much to my family who supported me in this long, oversea and sometimes difficult journey: Alessandro, Carla, Guido, Michela, Claudio and Alice; it is because of you that I never gave up.

TABLE OF CONTENTS

PART 1. INTRODUCTION AND AIMS

Chapter 1 Background and Introduction

Chapter 2 Non-invasive Assessment of Intracranial Pressure

PART 2. NON-INVASIVE INTRACRANIAL PRESSURE IN THE EXPERIMENTAL SETTINGS

Chapter 3 Doppler Non-invasive Monitoring of ICP in an Animal Model of Acute Intracranial Hypertension.

PART 3. NON-INVASIVE INTRACRANIAL PRESSURE IN THE INTRAOPERATIVE SETTINGS

Chapter 4 Intraoperative non-invasive ICP monitoring during pneumoperitoneum: a case and case report series

Chapter 5 Effects Of Prone Position And Positive End Expiratory Pressure On Intracranial Pressure In Patients Undergoing Spinal Surgery Using Different Non-Invasive Methods

Chapter 6 Effects Of Pneumoperitoneum And Trendelenburg Position On Intracranial Pressure Assessed Using Different Non-Invasive Methods

PART 4. NON-INVASIVE INTRACRANIAL PRESSURE IN NEUROINTENSIVE CARE

Chapter 7 The Accuracy Of Transcranial Doppler In Excluding Intracranial Hypertension Following Acute Brain Injury: A Multicenter Prospective Pilot Study

Chapter 8 Optic Nerve Sheath Diameter On Computed Tomography Is Correlated With Simultaneously Measured Intracranial Pressure In Patients With Severe Traumatic Brain Injury

Chapter 9 Ultrasound Non-Invasive Measurement Of Intracranial Pressure In Neurointensive Care: A Prospective Observational Study

Chapter 10 Optic Nerve Sheath Diameter Ultrasonography At Admission As Predictor Of Intracranial Hypertension And Impaired Autoregulation In Traumatic Brain Injured Patients

Chapter 11 Ultrasound Based Non-Invasive Intracranial Pressure In Children: A Pilot Study

PART 5. SUMMARY AND GENERAL DISCUSSION

LIST OF FIGURES

Figure 1.1. Example of extradural hemorrhage consequent to the insertion of invasive ICP _____ 21

Figure 1.2. Representation of the systolic (FV_s) and diastolic (FV_d) components of the spectral cerebral blood flow (CBF) velocity (FV) waveform. _____ 22

*Figure 1.3. Schematic representation of the acoustic windows for transcranial Doppler ultrasonography.*____ 23

Figure 1.4. Schematic representation of cerebral spinal fluid circulation. _____ 24

Figure 1.5. Magnetic Resonance imaging of the optic nerve and optic nerve sheath diameter. _____ 25

Figure 1.6. Measurement of ONSD with Ultrasound. _____ 26

*Figure 2.1. MRI method. A. A blood vessel MRI scout image showing the location of the axial plane for blood flow measurement (horizontal line). B. A Phase Contrast MRI image of blood flow through that location of carotid arteries, vertebral arteries and jugular veins. Black pixels indicate arterial inflow and white are venous outflow. C. Anatomical mid-sagittal T1 weighted MR image showing the location of the axial plane used for CSF flow measurement (horizontal line). D. MRI images of the region of interest for CSF flow: the spinal canal (light grey) and the spinal cord (dark grey). E-F. MRI-based measurements of arterial inflow, venous outflow (E), and cerebrospinal fluid flow (F) used for derivation of the MRICP with derived waveforms of the total arterial inflow and venous outflow (E) and CSF flow and arterial minus venous (F) during the cardiac cycle (with permission from Alperin et al.).*_____ 36

Figure 2.2. Measurement of ONSD. A: Methodology to measure ONSD on Magnetic Resonance. The axial proton density/T2-weighted turbo spin-echo fat-suppressed sequence is used to measure ONSD and optic nerve diameter B: Ultrasonographic picture of the optic nerve system. Caliper identifies the site of ONSD measurement 3 mm behind the retina. C: Computed Tomography image of the optic nerve sheath. Using electronic calipers ONSD is measured 3 mm behind and in a perpendicular vector with reference to the orbit. 38

Figure 2.3. A schematic representation of the communication between the subarachnoid space and the inner ear through the cochlear aqueduct. _____ 43

Figure 2.4. Non-invasive two-depth TCD device for absolute ICP measurements. _____ 47

Figure 2.5. Flowchart. Proposal of for invasive or non-invasive monitoring of ICP in traumatic brain injured patients at arrival in Emergency Department. Beside clinical assessment and brain CT we propose a possible use of a combination of the non-invasive techniques to screen patients where there is doubt on the need for invasive ICP/ CPP methods to monitoring patients, when the indications for an invasive method are not completely met or when an invasive method is contraindicated or not available. _____ 55

Figure 3.1. Traces displaying examples of experiments for each formula. In the examples is shown progressive intracranial hypertension owing to infusion of Hartmann’s solution into the lumbar subarachnoid space at an increasing rate, at last stage reaching 0.15 mL/min. _____ 74

Figure 3.2. Scatter plots of 1 minute averaged measured ICP versus aaICP (left upper panel) gPI (right upper panel) and FdICP (lower panel) (n=1344). Each of the three non-invasive ICP estimators showed a statistically significant positive relationship with measured ICP when each 1-minute sample of ICP and non-invasive ICP is considered as an independent sample. _____ 75

Figure 3.3. Non-invasive ICP methods receiver operating characteristic (ROC) of FVdICP (on the left), aaICP (middle panel), and gPI (left panel) and dichotomised with ICP above and below 20 mmHg of thresholds. _____ 77

Figure 4.1. Magnetic Resonance Imaging of the patient described in our case report. _____ 91

Figure 5.1. On the left panel, univariate Receiving Operator Curve (ROC) analysis for the supination/pronation status the different non-invasive parameters. On the right panel, univariate ROC analysis taking in account the use of PEEP. _____ 122

Figure 5.2. Cutoff value for mean ONSD to distinguish the mean ONSD value between supine and prone. The method showed a specificity of 75.0 and a sensitivity of 86.7 0, supine without PEEP; 1, prone without PEEP. _____ 123

Figure 6.1. Distribution of optic nerve sheath diameter (ONSD) (A), ICP measured with ICP_{Fvd} formula (B) and with ICP_{PI} (C) values measured at each time point. _____ 139

Figure 6.2. Univariate Receiving Operator Curve (ROC) analysis of the different non-invasive parameters. On the upper left panel (A), univariate ROC analysis taking in account the use PP (B versus PP); in the upper right panel (B), it takes in account the concomitant application of PP and Trendelenburg position (B versus TP+PP). In the lower panel (C), it takes in account the changes in ICP occurring between PP and the application of Trendelenburg position (PP versus TP+PP). Considering time points B versus PP and B versus TP+PP, ICP_{Fvd} presented the highest AUC value. Assessing the effects of application of Trendelenburg position after PP (PP versus TP+PP), ONSD showed to have the highest AUC compared to ICP_{Fvd} and ICP_{PI} (see table 6.2). ____ 141

Figure 7.1. Dichotomized ICP readings, ≤ 20 mmHg vs > 20 mmHg, ≤ 24.8 mmHg vs > 24.8 mmHg. _____ 159

Figure 7.2. Estimated conversion between ICP_{tcd} and ICP_i ; slope value = 1.02 (95% CI 0.85-1.36). _____ 160

Figure 7.3. Bland Altman plot showing mean bias of + 6.2 mmHg for ICP_{tcd} compared to ICP_i , with an agreement range from -5.6 to 18 mmHg. _____ 160

Figure 7.4. ROC curve analysis for ICP_{tcd} averaged over times (TIME1, TIME2, and TIME3) showing an AUC of 96.0% (95% CI 89.8%-100%). The estimated best threshold value was at an ICP_i of 24.8 mmHg corresponding to a sensitivity of 100% and a specificity of 91.2%. _____ 161

Figure 8.1. Scatterplot of ICP (mmHg) and ONSD (mm). The solid line is the linear prediction from the univariable regression. The short-dashed lines are the 95% confidence intervals for the linear prediction. The long-dashed lines are the 95% prediction interval for ICP given ONSD. _____ 179

Figure 8.2. Receiver operating curve (ROC) for ONSD on the risk of developing intracranial hypertension ($ICP \geq 20$ mmHg). It is a plot of the true positive rate (sensitivity) vs. the false positive rate ($1 - \text{specificity}$) at various thresholds of ONSD. The area under the curve is a measure of the diagnostic accuracy for ONSD of predicting intracranial hypertension. The dotted line represents a test which is no better than chance. _____ 180

Figure 9.1. Scatterplot of intracranial pressure (ICP, mmHg) and different non-invasive ICP estimators between patients (N=64). (A) optic nerve sheath diameter method (ONSD, $R=0.76$); (B) flow velocity systolic in the straight sinus, (FV_{sv} , $R=0.72$); (C) combination between ONSD and FV_{sv} ($nICP_{ONSD+FV_{sv}}$, ($R=0.80$)). Dark grey shaded areas on the plots represent 95% confidence intervals for the linear regressions; light grey shaded areas on the plots represent the 95% prediction interval for the linear regressions. _____ 196

ULTRASOUND BASED NON-INVASIVE INTRACRANIAL PRESSURE

Figure 9.2. Receiver operating characteristic (ROC) analysis for different non-invasive ICP predictors for a threshold of ICP ≥ 20 mmHg. (A) optic nerve sheath diameter method (ONSD); (B) systolic flow on the straight sinus (FV_{sv}); (C) the method based on the combination of ONSD and FV_{sv} ($nICP_{ONSD+FV_{sv}}$). The values shown on the curve in (A) and (B) represent the best thresholds (cut-off values presenting the best sensitivity and specificity (in brackets)) for prediction of intracranial hypertension (ICP ≥ 20 mmHg), respectively for ONSD and FV_{sv} . AUC is presented followed by 95% confidence intervals. _____ 198

Figure 9.3. Boxplots of the analysis of variance of ICP (A) and ONSD (B) between patients who survived and those who died. The mean ONSD between patients who survived and died was significantly different. _____ 200

Figure 10.1. Admission ONSD (in mm) as related to mean ICP (panel A), “dose” of ICP above 20 mm Hg (panel B) and mean PRx over whole monitoring period (panel C). The blue line represents the linear regression, and the shaded area the 95% confidence interval. _____ 214

Figure 10.2. Comparison of ONSD predicted ICP and measured ICP on admission to the NCCU after severe TBI (A – scatterplot, B – Bland Altman plot). _____ 215

Figure 10.3. Admission ONSD on US in patients who died and survived after severe TBI. _____ 215

Figure 11.1. Scatterplot of intracranial pressure (ICP, mmHg) and different non-invasive ICP estimators between patients. (A) ICP-derived optic nerve sheath diameter method ($nICP_{ONSD}$, $R=0.76$); (B) ONSD showed a correlation with ICP of 0.852 ($p<0.0001$). (C) $nICP_{FVd}$ method showed a correlation of $R=0.441$ ($p<0.0001$) and (D) Pia the weakest correlation with ICP ($R=0.321$, $p<0.001$); light grey shaded areas on the plots represent the 95% prediction interval for the linear regressions. _____ 231

Figure 11.2. Behaviour over time of ONSD (in mm, black line) and invasive ICP (in mmHg, grey line) for each patient included in the analysis. ONSD and ICP show to have a similar trend in all cases. _____ 232

Figure 11.3. Bland-Altman plots for different non-invasive ICP methods. Left panel represents the Bland-Altman analysis considering $nICP$ formula, that shows a bias of -5.00 mmHg, with 95% CI for ICP prediction of. 95% CI for prediction of 8.25 mmHg, and $95\%CI = 16.26$ mmHg for $nICP_{FVd}$ (right panel). _____ 233

Figure 11.4. Receiver operating characteristic (ROC) analysis for optic nerve sheath diameter method (ONSD). The values shown on the curve in the left and right panel represent the best thresholds (cut-off values presenting the best sensitivity and specificity [in brackets]) for prediction of intracranial hypertension (ICP) >15 mmHg (left panel) and >20 mmHg, right panel. AUC is presented followed by 95% confidence intervals. _____ 233

LIST OF TABLES

Table 2.1. Detection of increased ONSD compared to invasive and non-invasive methods. _____ 40

Table 2.2. Characteristics of the nICP methods. _____ 53

Table 3.1. Correlation with measured ICP, standard deviation (SD) , BIAS and 95% CI (mmHg) within every rabbit for each formula. FVd formula shows the best correlation coefficient (0.85) with invasive ICP and the lowest systemic error value. Aaslid formula demonstrated generally a good capability to detect ICP changes, but shows the greatest 95% CI and BIAS. gPI showest the smallest correlation coefficient and intermediate 95% CI and BIAS. _____ 76

Table 3.2. Correlation coefficients assessing the difference (Δ) between the three methods and invasive ICP in three different periods of infusion test. To= baseline, before the beginning of infusion test; T1=when Cushing Response begins; T2=maximum peak of ICP. The correlation coefficient measured with FdICP shows a statistically significant value in all the three periods, demonstrating that this is the best method to detect changes in ICP. Aaslid Formula seems to have a better performance during the pre CR period, and gPIInICP didn't show any statistically significant correlation with ICP at any point of measurement. _____ 78

Table 4.1. Intraoperative non-invasive ICP monitoring during pneumoperitoneum: a case and case report series. _____ 93

Table 4.2. Reports and studies on TCD monitoring for noninvasive ICP assessment during pneumoperitoneum. _____ 95

Table 4.3. _____ 99

Table 5.1. Demographic and surgical data of the patients. _____ 117

Table 5.2. variation of the different parameters at the different anesthesia timepoints. _____ 118

Table 5.3. Fixed effect multivariate regression. Models have been corrected for confounding variables, namely age, sex, BMI, type and time of surgery, fluids administration, ASA classification and co-morbidities. F-values statistically significant are reported in Bold (p-values). _____ 120

Table 5.4. Two-way ANOVA assessing the effect of PP, PEEP and their interaction on different parameters. 121

Table 6.1. Median values (IQR) of the studied parameters at different time points. _____ 138

Table 6.2. Receiver Operator Characteristic (ROC) analysis. _____ 141

Table 7.1. General characteristics and admission diagnoses. _____ 157

Table 7.2. Invasive (ICPi) and Trans-Cranial Doppler (ICPtcd) intracranial pressure (ICP) measurements at study times. TIME 1: ICPtcd immediately before ICPi insertion; TIME 2: ICPtcd immediately after ICPi insertion; TIME 3: from 2 to 3 h following ICPi insertion. _____ 158

ULTRASOUND BASED NON-INVASIVE INTRACRANIAL PRESSURE

Table 8.1. Baseline characteristics of cohort SD = standard deviation; APACHE = Acute Physiology and Chronic Health Evaluation; IQR = interquartile range. _____ 177

Table 8.2. Regression table comparing three linear models with ICP as the dependent variable. The between-rater agreement for ONSD measurements as determined by ICC was 0.89 (95%CI: 0.83 to 0.93, $P < 0.001$). ICC between right and left ONSD measurements was 0.96 (95% CI: 0.93 to 0.98, $P < 0.001$). The mean ONSD was 6.7 mm (SD 0.75) and the mean ICP during CT was 21.3 mmHg (SD 8.4). Using simple linear regression, there was a linear correlation between ICP and ONSD ($r = 0.74$, $P < 0.001$) (Figure 8.1 and Table 8.2). Although there was a linear relationship between ONSD and RAP ($r = 0.35$, $P = 0.007$) there was considerable variability around the point estimate (data not shown). _____ 178

Table 9.1. Baseline characteristics of the patient cohort. _____ 193

Table 9.2. Median values and interquartile range (IQR) of the studied parameters. _____ 194

Table 9.3. Summary of the linear mixed effects models between ICP and the non-invasive estimators across all measurement points ($N = 445$). Full model accounts for random intercepts and slopes; null model accounts for random intercepts only. _____ 195

Table 9.4. Correlations between ICP and non-invasive estimators across all measurement points ($N = 445$) and for average values between patients ($N = 64$). _____ 197

Table 9.5. Summary of the 95% prediction and confidence intervals (\pm standard deviations) for the linear regression between ICP and non-invasive estimators between patients ($N = 64$). _____ 197

Table 9.6. Results of Receiver Operator Curve (ROC) analysis for ICP ≥ 20 mmHg considering all measurement points ($N = 445$). _____ 199

Table 9.7. Summary table describing the association between ICP, ONSD and mortality. _____ 199

Table 10.1. Median (IQR) values of the parameters analysed. _____ 213

Table 11.1. Characteristics of the patients included in the study. _____ 229

Table 11.2. Median (IQR) values of the assessed variables. _____ 230

LIST OF MAIN ABBREVIATIONS

ABP, arterial blood pressure
ABP_d, diastolic arterial blood pressure
ABP_s, systolic arterial blood pressure
ACA, anterior cerebral artery
ARI, autoregulation index
BMI, body-mass index
CBF, cerebral blood flow
CI, confidence interval
CO₂, carbon dioxide
CPP, cerebral perfusion pressure
CPP_{opt}, optimal cerebral perfusion pressure
CSF, cerebrospinal fluid
CT, computed tomography
CVR, cerebrovascular resistance
EEG, electroencephalogram
ETCO₂, end-tidal carbon dioxide concentration
FV, cerebral blood flow velocity
FV_d, diastolic cerebral blood flow velocity
FV_s, systolic cerebral blood flow velocity
GCS, Glasgow coma scale
HR, heart rate
ICA, internal carotid artery
ICH, intracranial hypertension
ICP, intracranial pressure
IQR, interquartile range
LP, lumbar puncture
MCA, middle cerebral artery
MRI, magnetic resonance imaging
MS, midline shift
NCCU, Neurosciences Critical Care Unit
nCPP, non-invasive cerebral perfusion pressure
nICP, non-invasive intracranial pressure
nICP_{BB}, non-invasive intracranial pressure based on the black box method
nICP_{FV_d}, non-invasive intracranial pressure based on the diastolic cerebral blood flow velocity method
nICP_{CrCP}, non-invasive intracranial pressure based on the critical closing pressure method
nICP_{PI}, non-invasive intracranial pressure based on the pulsatility index method
NPV, negative predictive value
ONSD, optic nerve sheath diameter
OR, odds ratio

PaCO₂, partial pressure of carbon dioxide
PCA, posterior cerebral artery
PE, prediction error
PECO₂, pressure of expired carbon dioxide
PI, pulsatility index
PPV, positive predictive value
PRx, pressure reactivity index
R, correlation coefficient
R², coefficient of determination
REC, research ethics committee
RI, resistance index
ROC, receiver operating characteristic
rSCO₂, regional cerebral oxygen saturation
SAH, subarachnoid haemorrhage
SD, standard deviation
SDE, standard deviation of the error
TBI, traumatic brain injury
TCD, transcranial Doppler ultrasonography

SUMMARY

Intracranial pressure (ICP) is an important monitoring modality in the clinical management of several neurological diseases carrying the intrinsic risk of potentially lethal intracranial hypertension (ICH). Considering that the brain is in an enclosed compartment, ICH leads to brain hypoperfusion and eventually ischaemia followed by irreversible neuronal damage. Traumatic brain injury (TBI), for instance, is a condition in which ICH is strongly associated with unfavourable outcome and death.

Although ICP can guide patient management in neurocritical care settings, this parameter is not commonly monitored in many clinical conditions outside this environment. The invasive character of the standard methods for ICP assessment and their associated risks to the patient (like infections, brain tissue lesions, haemorrhage) contribute to this scenario. Such risks have prevented ICP assessment in a broad range of diseases like in patients with risk of coagulopathy, as well as in other conditions in which invasive assessment is not considered or outweighed by the risks of the procedure. Provided that knowledge of ICP can be crucial for the successful management of patients in many sub-critical conditions, non-invasive estimation of ICP (nICP) may be helpful when indications for invasive ICP assessment are not met and when it is not immediately available or even contraindicated.

Several methods for non-invasive assessment of ICP (nICP) have been described so far. Transcranial Doppler (TCD), for instance, is primarily a technique for diagnosing various intracranial vascular disorders such as emboli, stenosis, or vasospasm, but has been broadly utilised for non-invasive ICP monitoring due to its ability to detect changes in cerebral blood flow velocity derived from ICP variations. Moreover, TCD allows monitoring of these parameters as they may change in time.

Optic nerve sheath diameter ultrasonography (ONSD) is another non-invasive tool which gained interest in the last years. The optic nerve sheath is in continuous with the subarachnoid space, and when ICP increased, the diameter of ONSD enlarges proportionally to ICP.

The focus of this thesis is on the assessment, applications and development of ultrasound-based for nICP assessment in different clinical conditions where this parameter is relevant but in many circumstances not considered, including TBI and other neurological diseases

associated with impairment of cerebral blood flow circulation. As main results, ONSD and TCD-based non-invasive methods could replicate changes in direct ICP across time confidently, and could provide reasonable accuracy in comparison to the standard invasive techniques. These findings support the use of ultrasound based non-invasive ICP methods in a variety of clinical conditions requiring management of intracranial pressure and brain perfusion. More importantly, the low costs associated with nICP methods, ultrasound machines are widely available medical devices, could contribute to its widespread use as a reliable alternative for ICP monitoring in everyday clinical practice.

Chapter 1 . Background and Introduction

INTRACRANIAL PRESSURE MONITORING

The concept of intracranial pressure (ICP) was first described in 1783 by the Scottish anatomist Alexander Monro, who described the skull as a rigid structure containing incompressible brain and stated that a constant drainage of venous blood is required to allow continuous arterial supply (1,2). These assumptions were later confirmed in autopsy studies by George Kellie of Leith (3), whose findings were postulated as the Monro-Kellie doctrine. The doctrine was modified throughout the years with contributions of Vesalius (description of fluid-filled brain ventricles), François Magendie (establishment of the concept of cerebrospinal fluid – CSF (4)), George Burrows (reciprocal relationship between the volumes of CSF and blood (5)). However, it was Harvey Cushing in 1926 (6), who formulated the classic explanation of the doctrine: with an intact skull, the volume of the brain, blood, and CSF is constant; an increase in one component will cause a decrease in one or both of the other components.

On the basis of the Monro-Kellie doctrine, intracranial pressure can be described as the summation of at least four components, driven by different physiological mechanisms (7). The first component is associated with arterial blood inflow and volume of arterial blood. Most common phenomenon associated with this component is plateau wave of ICP. Second component of ICP is associated with venous blood outflow. Obstructions to the outflow of blood leads to elevation of ICP (like venous compression due to wrong head position, but also venous thrombosis). Third component is related with cerebrospinal fluid (CSF) circulation derangements, as commonly seen in ‘acute hydrocephalus’ after traumatic brain injury (TBI) or subarachnoid haemorrhage (SAH). In neurocritical care, this component is commonly eradicated by extraventricular drainage. Finally, the fourth component is related to increase in brain volume (oedema) or volume of contusion (like haematoma). Osmotherapy or surgical decompression is commonly used to eradicate this component. In clinical practice, it is important not only to monitor absolute value of ICP, but also to recognize which component is responsible for observed intracranial hypertension, as clearly different measures are appropriate for controlling different components (8).

ICP monitoring is one of the standard protocols that can guide patient management undergoing neurocritical care (9). In association with mean arterial blood pressure (ABP), ICP monitoring provides the knowledge of cerebral perfusion pressure ($CPP = ABP - ICP$),

interpreted as the main force maintaining cerebral blood flow (CBF). However, ICP/ CPP are not commonly considered in many clinical conditions outside neurocritical care settings or in non-specialized centres. The invasiveness of the standard methods for ICP monitoring (epidural, subdural, intraparenchymal and intraventricular monitors) and their associated risks to the patient (infections, brain tissue lesions, haemorrhage) contribute to this scenario (Figure 1). They have prevented ICP monitoring in a broad range of diseases, like in patients with risk of coagulopathy, as well as in other conditions in which invasive monitoring is not considered or outweighed by the risks of the procedure. Another downside is related to costs and availability: invasive monitoring is an expensive technique, requires trained personnel and neurosurgical settings. Average cost of intraparenchymal microtransducer is US\$ 600, additionally to US\$ 6000-10000 for the display monitor (10), which makes it inaccessible in low to middle income regions. Provided that knowledge of ICP can be crucial for the successful management of patients in many sub-critical conditions, non-invasive estimation of ICP may be helpful when indications for invasive ICP monitoring are not met and when it is not immediately available or even contraindicated.

Several methods for non-invasive assessment of ICP have been described so far: transcranial Doppler ultrasonography (TCD) to measure cerebral blood flow velocity indices (11); skull vibrations (12); brain tissue resonance (13); transcranial time of flight (14); venous ophthalmodynamometry (15); optic nerve sheath diameter assessment (ONSD) (16); tympanic membrane displacement (17,18); otoacoustic emissions (19); magnetic resonance imaging (MRI) to estimate intracranial compliance (20); ultrasound-guided eyeball compression (21), and recordings of visual evoked potentials (22).

Most of these methods are better suited for one-point assessment of instant value of ICP rather than continuous monitoring. TCD, on the other hand, has been widely explored as a tool for non-invasive ICP monitoring (23–37) due to its ability to detect changes in CBF with ample time resolution



Figure 1.1. Example of extradural hemorrhage consequent to the insertion of invasive ICP

Transcranial Doppler ultrasonography

Transcranial Doppler ultrasonography (TCD) technique is based on the phenomenon called Doppler effect, observed by the physicist Christian Andreas Doppler in the 19th century. This principle applied to imaging blood vessels was popularised by Reid and Spencer in the 1970's (38). The application of TCD in clinical practice was first described by Rune Aaslid and collaborators in 1982 (39) as a technique applying ultrasound probes for dynamic monitoring of CBF and vessel pulsatility in the basal cerebral arteries.

The Doppler effect states that when a sound wave with a certain frequency strikes a moving object, the reflected wave undergoes a change in frequency (the Doppler shift, f_d) directly proportional to the velocity of the reflector. When translated to medical applications, this principle has been applied to monitor erythrocyte motion inside an insonated blood vessel by measuring the difference in ultrasound frequencies between emission and reception (39). The equation derived from this principle is the basis for calculating cerebral blood flow velocity (FV, in cm/s) with TCD:

Equation 1.1

$$v = \frac{(c \times f_d)}{2 \times f_0 \times \cos \theta} \quad (1.1)$$

where c is the speed of the incident wave, f_0 is the incident pulse frequency, and θ is the angle of the reflector relative to the ultrasound probe (40).

TCD relies on pulsed wave Doppler to image vessels at various insonation depths. Received echoes generate an electrical impulse in the ultrasound probe and are processed to calculate f_d and v , yielding a spectral waveform with peak systolic velocity (FV_s) and end diastolic velocity (FV_d) values (Figure 2).

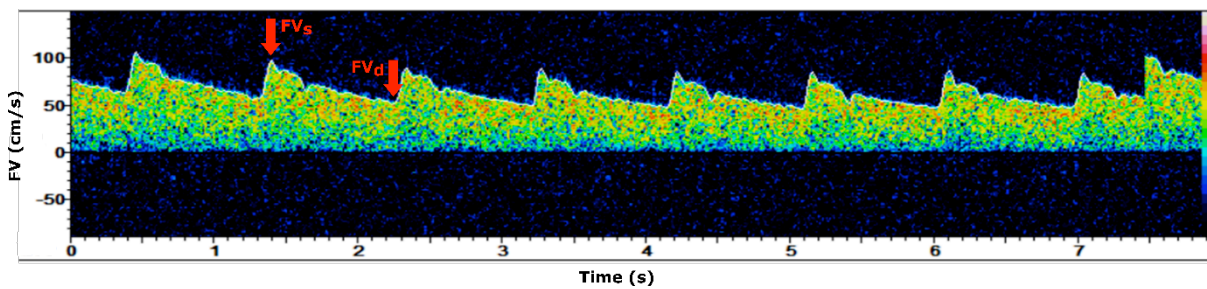


Figure 1.2. Representation of the systolic (FV_s) and diastolic (FV_d) components of the spectral cerebral blood flow (CBF) velocity (FV) waveform.

The use of low frequency ultrasound probes (≤ 2 MHz) allows insonation of basal cerebral arteries through different acoustic windows in the skull. These are regions presenting thin bone layers, through which ultrasound waves can be transmitted. There are four acoustic windows: transtemporal, transforaminal, transorbital and submandibular (Figure 3). The transtemporal window is the most frequently used, anatomically located above the zygomatic edge between the lateral canthus of the eye and auricular pinna. It allows insonation of the circle of Willis, specifically middle (MCA), anterior (ACA), posterior cerebral arteries (PCA), and terminal internal carotid artery (ICA) (41). Artery insonation is subject to probe angle, depth and appropriate acoustic window. However, inadequate transtemporal windows have been reported in 10-20% of patients (42,43). This has been associated with patient age, female sex, and other factors affecting the bone thickness (44).

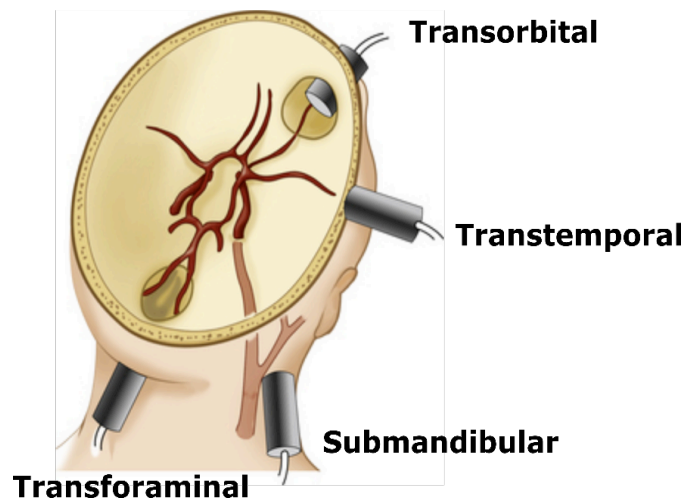


Figure 1.3. Schematic representation of the acoustic windows for transcranial Doppler ultrasonography.

In clinical practice, the MCA is the most frequently assessed artery. It is responsible for the greatest blood inflow to the brain (80%) (45,46), thus MCA measurement may represent the global blood flow. CBF represents the blood supply to the brain in a given period of time, and global changes in this parameter can be monitored continuously and non-invasively using TCD-derived FV (47). However, FV is only proportional to CBF when vessel cross-sectional area and angle of insonation are constant. The velocity detected by the probe as a fraction of the real velocity depends on the cosine of the angle of insonation (Equation 1.1). Consequently, at 0 angle, erythrocytes velocities are equal (cosine of $\theta = 1$), whereas at 90 degrees, no detection of velocity is possible. Anatomically, MCA insonation at the transtemporal acoustic window only allows signal capture at narrow angles (<30 degrees), which approximates the detected velocity of the true velocity (87% to 100%) (48).

Non-invasive estimation of ICP and CPP

TCD waveform analysis has been investigated as a technique for non-invasive estimation of ICP (nICP) and CPP (nCPP). TCD-derived nICP/nCPP methods are based on the relationship between ICP/ CPP and indices derived from cerebral blood flow velocity.

Applications of TCD for nICP monitoring are conceivable if one considers the insonated compliant MCA as a biological pressure transducer, whose walls can be deflected by

transmural pressure (equivalent to CPP), modulating accordingly the FV pulsatile waveform (37).

Optic Nerve Sheath Diameter (ONSD) Ultrasonography for assessment of ICP

The optic nerve sheath is continuous with the meninges of the central nervous system and is encased with the subarachnoid membrane (Figure 3.4 and 3.5) (37,38). Cerebrospinal fluid (CSF), located in the subarachnoid space, accumulates in the optic nerve sheath thereby widening its diameter in the response to increased ICP and limited intracranial compliance.

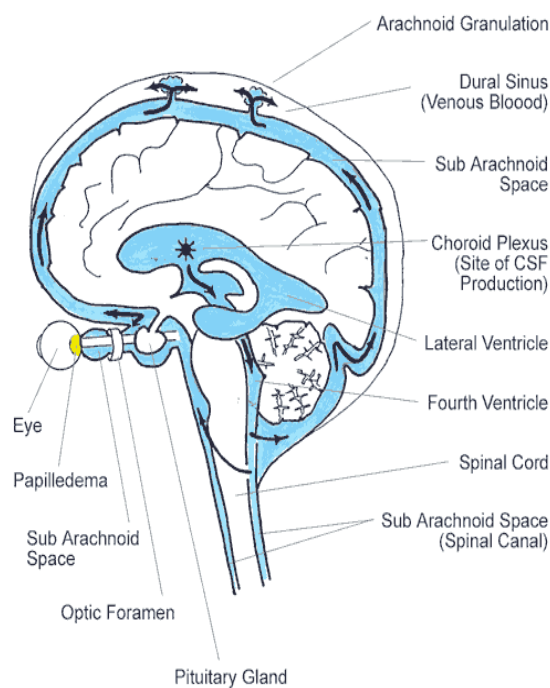


Figure 1.4. Schematic representation of cerebral spinal fluid circulation.

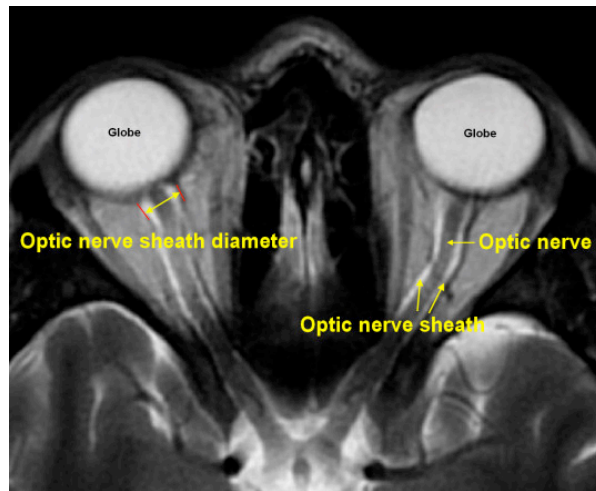


Figure 1.5. Magnetic Resonance imaging of the optic nerve and optic nerve sheath diameter.

Ultrasonography of ONSD has been shown to correlate with increased ICP (Figure 3.6) (37-40). Alternatively, ONSD measurements on MRI and CT are strongly correlated with increased ICP, but the relationship between optic nerve sheath diameter (ONSD) measured radiologically and simultaneously measured intracranial pressure (ICP) in patients with intracranial hypertension is not clear.

In this project, the changes of ONSD during recorded wave of ICP in NCCU will be analysed with ICP transducer in-situ. We intend to evaluate what is dynamics of ONSD changes in comparison to direct ICP monitoring in patients with intracranial hypertension in different clinical pathologies (traumatic brain injury, stroke, subarachnoid haemorrhage).

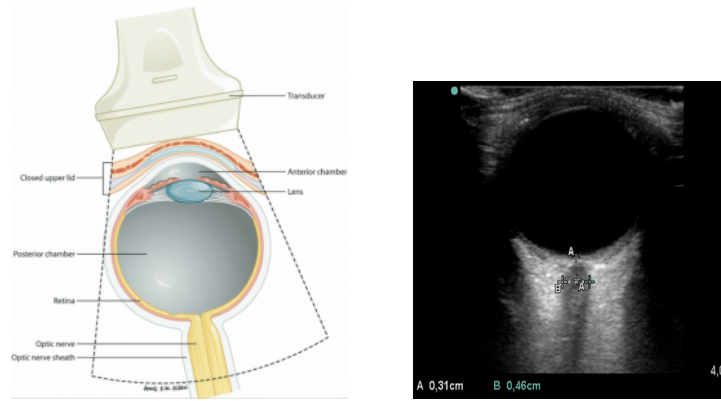


Figure 1.6. Measurement of ONSD with Ultrasound.

AIMS:

This project is organized into three general objectives:

OBJECTIVE 1. Evaluation of TCD-based methods versus invasive ICP

TCD-based, model-derived secondary indices offer readily available means for assessment and real-time monitoring of physiological and pathological processes, facilitating detection of onset of breakdown of homeostasis of cerebral and cerebrospinal circulation and estimation of ICP.

OBJECTIVE 2. To evaluate the dynamics of ICP versus ONSD methods

To determine the association between simultaneously obtained ONSD measured on CT, Ultrasound and ICP in patients with severe intracranial hypertension. In addition, to determine the ability of ONSD to discriminate between intracranial hypertension (ICP ≥ 20 mmHg vs. ICP < 20 mmHg).

OBJECTIVE 3. To investigate the comparison and utilisation of both techniques

The last part of my project was concentrated on the comparison between TCD-based methods and OSND methods and on the study of an innovative system of non-invasive ICP monitoring

using a combination of these techniques and verifying their accuracy and feasibility in patients with intracranial hypertension.

OUTLINE OF THE THESIS

These general aims have been translated in a series of experiments, retrospective analyses and background studies which are presented in the subsequent chapters of this thesis.

Chapter 2 provides a further clinical background for the evaluation of non-invasive intracranial pressure in patients with traumatic brain injury, subarachnoidal haemorrhage, and stroke. We describe the application of different techniques and methods to measure non-invasive ICP, through an historical description of the current available methods used in the experimental and clinical practice.

Chapter 3 describes in an experimental model of intracranial hypertension during infusion studies the accuracy of different non-invasive methods to assess ICP using TCD Ultrasonography.

Chapter 4 provides the clinical background for the intraoperative use of TCD and ONSD during surgery involving pneumoperitoneum and Trendelenburg position highlighting the potential use of these techniques in the assessment of ICP during surgical procedures.

Chapter 5 introduces the use of Ultrasound based non-invasive ICP methods in the intraoperative settings and in particular the effects of prone position and of positive- end expiratory pressure on cerebral haemodynamics

Chapter 6 continues research in the intraoperative settings and in particular in patients undergoing Trendelenburg position and pneumoperitoneum. In particular, we tested the ability of non-invasive methods to assess changes in ICP during these procedures.

Chapter 7 describes in a multicenter pilot study, the application of non-invasive methods in brain injured patients and the ability of these methods to identify patients at risk of intracranial hypertension.

Chapter 8 introduces the role of ONSD in the assessment of intracranial hypertension in patients with traumatic brain injury.

Chapter 9 continues research into the role of ONSD and TCD in the estimation of ICP. In particular, we compared different Ultrasound based methods to assess the best estimator of ICP.

Chapter 10 describes the role of ONSD as predictor of increased intracranial pressure and impaired autoregulation and the relationship between ONSD and mortality in TBI patients.

Chapter 11 explores the application of Ultrasound based non-invasive ICP methods in the pediatric population.

Chapter 12 provides a summary of our findings and the possible future applications of ultrasound based non-invasive ICP.

REFERENCES

1. Monro, A. (1783). Observations on the structure and functions of the nervous system: illustrated with tables. Edinburgh.
2. Wilson, M.H. (2016). Monro-Kellie 2.0: The dynamic vascular and venous pathophysiological components of intracranial pressure. *J. Cereb. Blood Flow Metab.* 36, 1338–1350.
3. Kellie. (1824). Appearances Observed in the Dissection of Two Individuals; Death from Cold and Congestion of the Brain. *Tr. Med.-Chir. Soc. Edinburgh* 1.
4. Magendie, F. (1842). *Recherches anatomique et physiologique sur le liquide cephalo-rachidien ou cerebro-spinal.* Paris: Me' quignon-Marvis fils.
5. Burrows, G. (1848). *On Disorders of the Cerebral Circulation and on the Connection between Affections of the Brain and Diseases of the Heart.* Philadelphia, PA, USA: Lea & Blanchard.
6. Cushing, H. (1926). *The Third Circulation in Studies in Intracranial Physiology and Surgery.* London: Oxford University Press.
7. Czosnyka, M., and Pickard, J.D. (2004). Monitoring and interpretation of intracranial pressure. *J. Neurol. Neurosurg. Psychiatry* 75, 813–821.
8. Cardim, D., Robba, C., Donnelly, J., Bohdanowicz, M., Schmidt, B., Damian, M., Varsos, G. V, Liu, X., Cabeleira, M., Frigieri, G., Cabella, B., Smielewski, P., Mascarenhas, S., and Czosnyka, M. (2015). Prospective study on non-invasive assessment of ICP in head injured patients: comparison of four methods. *J. Neurotrauma* .
9. Carney, N., Totten, A.M., O'Reilly, C., Ullman, J.S., Hawryluk, G.W.J., Bell, M.J., Bratton, S.L., Chesnut, R., Harris, O.A., Kissoon, N., Rubiano, A.M., Shutter, L., Tasker, R.C., Vavilala, M.S., Wilberger, J., Wright, D.W., and Ghajar, J. (2016). *Guidelines for the Management of Severe Traumatic Brain Injury, Fourth Edition.* *Neurosurgery* 19, 1.
10. Surgeons., B.T.F.A.A. of N.S.C. of N. (2007). *Guidelines for the Management of Severe Traumatic Brain Injury 3rd Edition.* *J. Neurosurg.* 24, Suppl, S1-106.
11. Hanlo, P.W., Peters, R.J.A., Gooskens, R.H.J.M., Heethaar, R.M., Keunen, R.W.M., Van Huffelen, A.C., Tulleken, C.A.F., and Willemsse, J. (1995). Monitoring intracranial dynamics by transcranial Doppler - A new Doppler index: Trans Systolic Time. *Ultrasound Med. Biol.* 21, 613–621.
12. Ueno, T., Ballard, R.E., Shuer, L.M., Cantrell, J.H., Yost, W.T., and Hargens, A.R. (1998). Noninvasive measurement of pulsatile intracranial pressure using ultrasound. *Acta Neurochir. Suppl.* 71, 66–69.
13. Michaeli, D., and Rappaport, Z.H. (2002). Tissue resonance analysis; a novel method for noninvasive monitoring of intracranial pressure. Technical note. *J. Neurosurg.* 96, 1132–1137.
14. Ragauskas, A., Daubaris, G., Ragaisis, V., and Petkus, V. (2003). Implementation of non-invasive brain physiological monitoring concepts. *Med. Eng. Phys.* 25, 667–678.
15. Querfurth, H.W., Lieberman, P., Arms, S., Mundell, S., Bennett, M., and van Horne, C. (2010). Ophthalmodynamometry for ICP prediction and pilot test on Mt. Everest. *BMC Neurol.* 10, 106.
16. Geeraerts, T., Launey, Y., Martin, L., Pottecher, J., Vigué, B., Duranteau, J., and Benhamou, D. (2007). Ultrasonography of the optic nerve sheath may be useful for

- detecting raised intracranial pressure after severe brain injury. *Intensive Care Med.* 33, 1704–1711.
17. Reid, A., Marchbanks, R.J., Bateman, D.E., Martin, A.M., Brightwell, A.P., and Pickard, J.D. (1989). Mean intracranial pressure monitoring by a non-invasive audiological technique: a pilot study. *J. Neurol. Neurosurg. Psychiatry* 52, 610–612.
 18. Shimbles, S., Dodd, C., Banister, K., Mendelow, A.D., and Chambers, I.R. (2005). Clinical comparison of tympanic membrane displacement with invasive intracranial pressure measurements. *Physiol. Meas.* 26, 1085–1092.
 19. Frank, A.M., Alexiou, C., Hulin, P., Janssen, T., Arnold, W., and Trappe, A.E. (2000). Non-invasive measurement of intracranial pressure changes by otoacoustic emissions (OAEs)--a report of preliminary data. *Zentralbl. Neurochir.* 61, 177–80.
 20. Alperin, N.J., Lee, S.H., Loth, F., Raksin, P.B., and Lichtor, T. (2000). MR-Intracranial pressure (ICP): a method to measure intracranial elastance and pressure noninvasively by means of MR imaging: baboon and human study. *Radiology* 217, 877–85.
 21. Bartusis, L., Zakelis, R., Daubaris, G., Ragauskas, A., Rutkauskas, S., Matijosaitis, V., and Preiksaitis, A. (2012). Ophthalmic artery as a sensor for non-invasive intracranial pressure measurement electronic system. *Elektron. ir Elektrotechnika* 122, 45–48.
 22. Zhao, Y.L., Zhou, J.Y., and Zhu, G.H. (2005). Clinical experience with the noninvasive ICP monitoring system., in: *Acta Neurochirurgica, Supplementum*. pps. 351–355.
 23. Schmidt, B., Klingelhöfer, J., Schwarze, J.J., Sander, D., and Wittich, I. (1997). Noninvasive Prediction of Intracranial Pressure Curves Using Transcranial Doppler Ultrasonography and Blood Pressure Curves. *Stroke* 28, 2465–2472.
 24. Schmidt, B., Czosnyka, M., and Klingelhöfer, J. (2002). Clinical applications of a non-invasive ICP monitoring method. *Eur. J. Ultrasound* 16, 37–45.
 25. Bellner, J., Romner, B., Reinstrup, P., Kristiansson, K.A., Ryding, E., and Brandt, L. (2004). Transcranial Doppler sonography pulsatility index (PI) reflects intracranial pressure (ICP). *Surg. Neurol.* 62, 45–51.
 26. Figaji, A.A., Zwane, E., Fieggen, A.G., Siesjo, P., and Peter, J.C. (2009). Transcranial Doppler pulsatility index is not a reliable indicator of intracranial pressure in children with severe traumatic brain injury. *Surg. Neurol.* 72, 389–394.
 27. Kashif, F.M., Heldt, T., and Verghese, G.C. (2008). Model-based estimation of intracranial pressure and cerebrovascular autoregulation. *Comput. Cardiol.* 35, 369–372.
 28. Schmidt, B., Czosnyka, M., Schwarze, J.J., Sander, D., Gerstner, W., Lumenta, C.B., and Klingelhöfer, J. (2000). Evaluation of a method for noninvasive intracranial pressure assessment during infusion studies in patients with hydrocephalus. *J. Neurosurg.* 92, 793–800.
 29. Schmidt, B., Czosnyka, M., Raabe, A., Yahya, H., Schwarze, J.J., Sackerer, D., Sander, D., and Klingelhöfer, J. (2003). Adaptive noninvasive assessment of intracranial pressure and cerebral autoregulation. *Stroke* 34, 84–89.
 30. Asil, T., Uzunca, I., Utku, U., and Berberoglu, U. (2003). Monitoring of Increased Intracranial Pressure Resulting From Cerebral Edema With Transcranial Doppler Sonography in Patients With Middle Cerebral Artery Infarction. *J Ultrasound Med* 22, 1049–1053.
 31. Voulgaris, S.G., Partheni, M., Kaliora, H., Haftouras, N., Pessach, I.S., and Polyzoidis,

- K.S. (2005). Early cerebral monitoring using the transcranial Doppler pulsatility index in patients with severe brain trauma. *Med. Sci. Monit.* 11, CR49-R52.
32. Steinbach, G.C., Macias, B.R., Tanaka, K., Yost, W.T., and Hargens, A.R. (2005). Intracranial pressure dynamics assessed by noninvasive ultrasound during 30 days of bed rest. *Aviat. Sp. Environ. Med.* 76, 85–90.
 33. Prunet, B., Asencio, Y., Lacroix, G., Moncriol, A., Dagain, A., Cotte, J., Esnault, P., Boret, H., Meaudre, E., and Kaiser, E. (2012). Noninvasive detection of elevated intracranial pressure using a portable ultrasound system. *Am. J. Emerg. Med.* 30, 936–941.
 34. Kashif, F.M., Verghese, G.C., Novak, V., Czosnyka, M., and Heldt, T. (2012). Model-Based Noninvasive Estimation of Intracranial Pressure from Cerebral Blood Flow Velocity and Arterial Pressure. *Sci. Transl. Med.* 4, 129ra44-129ra44.
 35. Wakerley, B., Yohana, K., Luen Teoh, H., Tan, C.W., Chan, B.P.L., and Sharma, V.K. (2014). Non-invasive intracranial pressure monitoring with transcranial Doppler in a patient with progressive cerebral venous sinus thrombosis. *J. Neuroimaging* 24, 302–4.
 36. Wakerley, B.R., Kusuma, Y., Yeo, L.L.L., Liang, S., Kumar, K., Sharma, A.K., and Sharma, V.K. (2014). Usefulness of transcranial doppler-derived cerebral hemodynamic parameters in the noninvasive assessment of intracranial pressure. *J. Neuroimaging* , 1–6.
 37. Cardim, D., Robba, C., Bohdanowicz, M., Donnelly, J., Cabella, B., Liu, X., Cabeleira, M., Smielewski, P., Schmidt, B., and Czosnyka, M. (2016). Non-invasive Monitoring of Intracranial Pressure Using Transcranial Doppler Ultrasonography: Is It Possible? *Neurocrit. Care* .
 38. Helmke K, Burdelski M, Hansen HC. Detection and monitoring of intracranial pressure dysregulation in liver failure by ultrasound. *Transplantation.* 2000;70: 392–5. doi:Doi 10.1097/00007890-200007270-00029
 39. Komut E, Kozaci N, Sönmez BM, Yilmaz F, Komut S, Yildirim ZN, et al. Bedside sonographic measurement of optic nerve sheath diameter as a predictor of intracranial pressure in ED. *Am J Emerg Med.* 2016;34: 963–967. doi:10.1016/j.ajem.2016.02.012
 40. Moretti R, Pizzi B. Optic Nerve Ultrasound for Detection of Intracranial Hypertension in Intracranial Hemorrhage Patients Confirmation of Previous Findings in a Different Patient Population. 2009;21: 16– 22

Chapter 2 . Non-invasive assessment of intracranial pressure

Chiara Robba, Susanna Bacigaluppi, Danilo Cardim, Joseph Donnelly, Marek Czosnyka

Acta Neurol Scand. 2016 Jul;134(1):4-21.

ABSTRACT

Background: Monitoring of intracranial pressure (ICP) is invaluable in the management of neurosurgical and neurological critically ill patients. Invasive techniques (ventriculostomy and microtransducers) are considered the gold standard in terms of reliability in the measurement of ICP but are associated with certain risks. Thus, the availability of a valid method to noninvasively detect ICP increase is of great utility for managing these patients. This review provides a comparative description of the different methods for non-invasive ICP measurement.

Brain imaging techniques, based on morphological changes associated with ICP increases: Magnetic Resonance, Computed Tomography, and optic nerve sheath diameter assessment; indirectly transmitted ICP caption: fundoscopy, timpanic membrane displacement; cerebral flow change detection: transcranial doppler, eyeball ophthalmic artery method; monitoring of metabolic alterations: Near Infrared Spectroscopy; neurophysiological registrations of functional activity: electroencephalography, visual Evoked Potentials, oto-acoustic emissions, time of flight method.

At present, none of the noninvasive techniques available are suitable enough to be used alone as a substitute for invasive monitoring. However, following the present analysis and considerations upon each technique, we propose a possible flowchart based on the combination of non-invasive techniques including continuous TCD and repetitive US measurements of ONSD, which can offer either a support in identifying the necessity for an invasive monitoring or a quite useful tool for patients where invasive ICP is contraindicated at all or unavailable.

INTRODUCTION

Intracranial hypertension (IH) is an important cause of secondary brain injury, and its association with poor outcome has been extensively demonstrated (1). Several conditions are associated with IH, which can be classified into extracranial (fever, increased abdominal pressure, increase of intra-thoracic pressure, venous obstruction, hypercarbia, hypoxia) and intracranial causes (hematoma, contusion, cerebrospinal fluid (CSF) alterations or edema) (revised in (2)). ICP monitoring is crucial in the management of neurocritical patients as clinical signs of IH are tardive and have a poor performance in predicting elevated ICP (3).

According to ‘The Brain Trauma Foundation’ guidelines (4), invasive ICP monitoring is indicated in all severe TBI patients in the following conditions: either positive brain CT findings (hematomas, contusion, swelling, herniation, or compressed basal cisterns), or normal brain CT if the patient is older than 40 years, or in presence of systolic blood pressure below 90 mmHg or in case of abnormal flexion or extension in response to pain.

The gold standard for ICP measurement is invasive monitoring through an intraventricular catheter; however, this technique is associated with certain risks (5).

Non-invasive estimation of ICP may be helpful when indications for invasive ICP measurement are not met or when ICP monitoring is not immediately available or even contraindicated, as in case of coagulopathy. Pathologic IH is defined when ICP rises persistently above 20-25 mmHg.

The aim of this chapter is to review the current available modalities for non-invasive ICP measurement. We organized the various methods in categories, according to the pathophysiological mechanism used to detect ICP increase. In particular, we divided them in: *Brain imaging techniques*, (Magnetic Resonance (MR), Computed Tomography (CT), and Optic Nerve Shear Diameter (ONSD assessment)); *Indirectly transmitted ICP* (fundoscopy, tympanic membrane displacement (TMD)); *Cerebral Blood Flow change detection* (transcranial doppler (TCD), eyeball ophthalmic artery method); *Monitoring of metabolic alterations* (Near Infrared Spectroscopy (NIRS)); *Neurophysiological registrations of functional activity* (electroencephalography, (EEG) including visual Evoked Potential (VEP), otoacoustic emissions, time of flight (TOF) method).

ICP ESTIMATION THROUGH IMAGING

CT

A variety of CT findings have been considered for predicting elevated ICP: the midline shift, the size of sulci, the morphology of cisterns (6), and ventricles (7), intracerebral hematoma size, the presence of contusions or of subarachnoidal blood. However, none of these findings have demonstrated to be sufficiently reliable in assessing increased ICP (reviewed by (8)).

A normal brain CT at admission does neither exclude the risk of early ICH (9), nor the risk of following development of elevated ICP. Similar considerations were made regarding the predictive value of abnormal CT findings in the assessment of ICP (10). Some authors (11) attempted to create a CT based prediction model including ventricular size, sulci size, degree of transfalxine herniation, and gray/white matter differentiation, and they demonstrated that initial brain CT findings showed a linear, but ultimately non-predictive relationship with baseline ICP. This finding was also confirmed in another study based on the Marshall Brain CT classification (12) and by several other authors (6, 13-18).

In summary, brain CT is a valuable clinical tool for quickly diagnosing and managing patients presenting with clinical signs or symptoms of raised ICP. However, no Brain CT based criteria is sufficient, and this method has demonstrated high specificity but low sensitivity (11-14) with a high possibility of false-negatives (14, 16, 17).

MRI cerebrospinal fluid, volume accounting

The MRI based method to measure ICP takes advantage of the concept of intracranial elastance, derived from the exponential relationship between intracranial volume and pressure (19) (see figure 2.1).

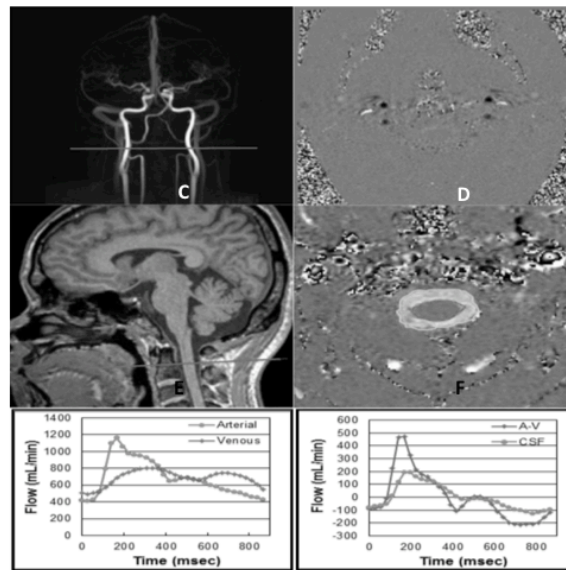


Figure 2.1. MRI method. *A.* A blood vessel MRI scout image showing the location of the axial plane for blood flow measurement (horizontal line). *B.* A Phase Contrast MRI image of blood flow through that location of carotid arteries, vertebral arteries and jugular veins. Black pixels indicate arterial inflow and white are venous outflow. *C.* Anatomical mid-sagittal T1 weighted MR image showing the location of the axial plane used for CSF flow measurement (horizontal line). *D.* MRI images of the region of interest for CSF flow: the spinal canal (light grey) and the spinal cord (dark grey). *E-F.* MRI-based measurements of arterial inflow, venous outflow (*E*), and cerebrospinal fluid flow (*F*) used for derivation of the MRICP with derived waveforms of the total arterial inflow and venous outflow (*E*) and CSF flow and arterial minus venous (*F*) during the cardiac cycle (with permission from Alperin et al.).

The pulsatility of blood flow with each cardiac cycle causes small fluctuation in intracranial volume, and the intracranial elastance is derived from the variation of these changes during the cardiac cycle. Thus, ICP value can be derived from the known relationship between ICP and elastance (20).

The accuracy of the MRI-based method was initially evaluated using a craniospinal flow-volume model, where the volume changes (Δ ICV) could be determined independently from the method (21).

This technique offered high accuracy, reproducibility and good temporal response of non-steady flow measurement with the cine phase contrast technique (average maximum Δ ICV value measured by MRI which within 5% of the value independently measured). Early evaluation of absolute ICP values of measurement reproducibility in human subjects

demonstrated a much larger measurement variability of 18% (22).

The relationship between time varying change in pressure was studied experimentally in animal model by Alperin et al. (22). The authors found a linear relationship between the amplitudes of the CSF pressure gradient measured by MRI and the amplitude of the invasively measured pulse pressure at three different levels of ICP.

Alperin et al. investigated the use of MR as a noninvasive method to assess intracranial elastance and pressure in patients with an invasive ICP measurement. From the ratio of pressure to volume change the elastance index was derived finding a very good correlation with invasive ICP ($r^2 = 0,965$; $p < 0.005$) (22). Moreover, Muehlmann et al. (23) found a positive correlation (Spearman Q = 0.64, P = 0.01) between shunt valve opening pressure and MR-ICP in 15 shunt-treated hydrocephalus children without signs of shunt malfunction.

This method has been successfully applied for ICP assessment in patients with cerebral arteriovenous malformations (with assessment of blood and CSF dynamics as well) (24) and as a prognostic tool in patients with symptomatic hydrocephalus (25). Moreover, MR derived ICP method was successfully applied to demonstrate that severity of headaches in acute mountain sickness is correlated with the change in ICP between normoxia and hypoxia (26).

However, this method cannot be used for continuous monitoring or repeated assessment of ICP over time and it requires a careful selection of representative image slides and the choice of the representative blood vessels (27).

OPTIC NERVE SHEATH DIAMETER

Anatomy and physiology

The sheath enveloping the optic nerve is in continuity with the dura mater of the brain and the subarchnoidal interspace filled with CSF, accounting for a direct connection between the two compartments (28). As the ONS is distensible, CSF pressure variations influence the volume of ONSD with fluctuations in the anterior, retro-bulbar compartment, about 3 mm behind the

globe (29). There is a linear relationship between peri-optic CSF pressure and ICP (6, 30), and ONSD changes almost directly with ICP (29, 31), as during osmotic therapy (32) or following CO₂ variations (33).

Thus, ONSD for ICP detection based either on CT, MR or ultrasound, has been studied by several authors (figure 2).

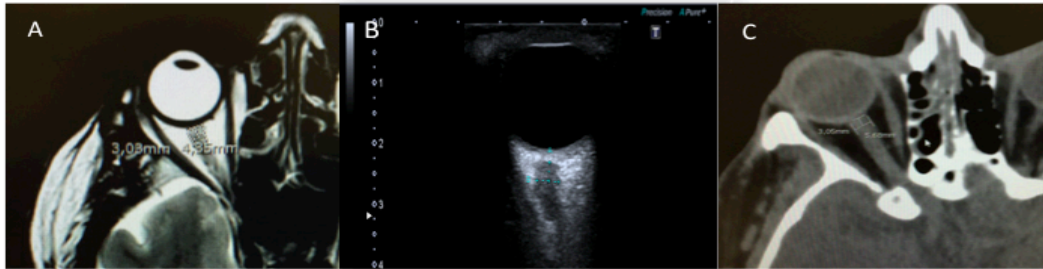


Figure 2.2. Measurement of ONSD. **A:** Methodology to measure ONSD on Magnetic Resonance. The axial proton density/T2-weighted turbo spin-echo fat-suppressed sequence is used to measure ONSD and optic nerve diameter **B:** Ultrasonographic picture of the optic nerve system. Caliper identifies the site of ONSD measurement 3 mm behind the retina. **C:** Computed Tomography image of the optic nerve sheath. Using electronic calipers ONSD is measured 3 mm behind and in a perpendicular vector with reference to the orbit.

ONSD and Ultrasound

Ultrasonography is a simple bedside tool, widely used in emergency units (34). Compared with CT and MR, ultrasound has low cost, high availability, does not need long acquisition times, does not require harmful patient transport and seems to have a high reproducibility of measures (29, 35, 36,37,38). However, due to its operator-dependency it should be combined with other clinical signs (37).

The cut-off value for normal ICP assessed with ONSD ranges from 4.8 to 6 mm. With exception of a study based on a very small sample size of TBI patients (38), all other studies found good correlation coefficients and good specificity and sensibility, demonstrating high accuracy for this method (as shown in table 2.1).

Ultrasound of the ONS has also been compared to findings of increased ICP on CT or MR, including the size of ventricle, basilar cistern, sulci, degree of transfalcine herniation, and gray/white matter differentiation (3, 39-41) and it appears much more reliable than these (42).

ONSD ranges from 4.84 to 6.4 mm in adult patients with radiological findings suggesting increased ICP and from 3.49 to 4.94 mm in patients with no radiological alterations, proving good sensitivity and specificity (table 2.1).

ONSD acquired with ultrasound has also been performed on children (29, 36): the upper limit of normality for children is considered 4.0 mm in infants aged less than 1 year, and 4.5 mm in elder children (36, 43, 44) with a rather good sensitivity (83%) despite a low and a specificity (38%) for predicting increased ICP .

ONSD in children has been investigated in different clinical scenarios associated with intracranial hypertension, such as acute hydrocephalus (44), intracranial lesions (39, 45) and liver failure (46); at present, there are no studies in the pediatric population which have compared ONSD values to direct ICP measurements.

Although this technique does not seem to be accurate enough to be used as a replacement for invasive ICP measuring methods, it has a good accuracy in recognizing normal from increased ICP.